Permanent Magnet Eddy Current Comparison of Surface Permanent Magnet Synchronous Motors with Different Permanent Magnet Shapes

Sun-Kwon Lee[1,2], Gyu-Hong Kang[1], *Senior Member IEEE* and Jin Hur[2], *Senior Member IEEE* and Byoung-Woo Kim[2]
[1]Korea Marine Equipment Research Institute, SongJeong-Dong, GangSeo-Gu, Busan, 1631-10, Korea
[2]Dept. of Electrical Engineering, University of Ulsan, 102. Street Dae-hak, Nam-gu, Ulsan 680-749, Korea
sunkwonlee@komeri.re.kr

***Abstract*—This paper presents the comparisons of permanent magnet (PM) eddy current of surface permanent magnet synchronous motor (SPMSM) with different rare-earth magnet shapes. The PM eddy current is analyzed to compare for each shape by 2 dimensional (2D) finite element analysis (FEA). The eddy current and their loss of particular position of PM are displayed for each model. The effect of partly enlarged air-gap made by PM shape to PM eddy current is studied.**

***Index Terms*—SPMSM, permanent magnet, eddy current, finite element analysis.**

I. Introduction

PM machines with a fractional number of slots per pole and a concentrated winding have shorter end windings and lower overall length and yet have high efficiency, torque, and power density [1]-[2]. In addition, not only copper loss but also copper cost can be downsized. On the other hand, the eddy current loss in the PM increases due to harmonic magnetic fields made by fractional slot pitch condition with concentrated winding [3]. The electric conductivity of sintered Nd-Fe-B magnet is very high, so the eddy current in PM increase. The temperature rise in PM especially partial area by eddy current loss can cause the partial demagnetization problem.

Some studies deal the eddy current loss analysis and reduction of PM with segmented magnet. The comparison of PM eddy current between interior permanent magnet (IPM) and SPM is also introduced [3]-[4]. The eddy current loss of PM for is calculated by analytical methods, and characteristics of magnet position are also discussed [5]. Seo and their colleagues introduced the loss characteristics of IPMSM using adaptive loss coefficients [6]. Yamazaki [7] investigated the PM eddy current loss variation according to stator and rotor shapes, but they are focused on PM types such as IPM, inset, and SPM.

In this paper, we investigated the PM eddy current effects of SPMSM with concentrated winding and fractional pole/slot combination by 2D FEA. The PM eddy current and their relationship to magnetic field characteristics are compared according to PM shape difference. The eddy current loss and magnetic field in particular PM position are also studied.

II. Analysis Model Descriptions

Fig. 1 shows the magnetic circuit structure of analyzed models. The identical stator with 12 slots concentrated windings is employed for each model, so the only difference between two models is PM shape. The detail descriptions of analyzed models are listed in Table I.

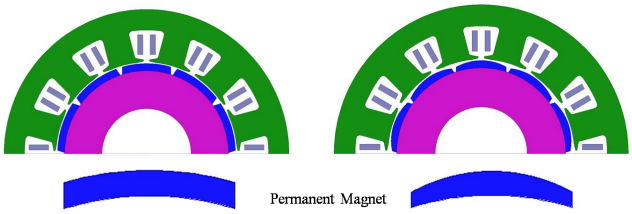

Fig. 1. Analysis models with different magnet shapes. (a) Model1, (b) Model2.

TABLE I
Specifications of Analyzed Models

Items	Values	Unit
Poles-slots	10 poles, 12 slots	-
Rotational speed	4000	rpm
Armature current	10	A
Stator Out Diameter	180	mm
Stack Length	54	mm
Residual Induction	1.21	T
Magnet type	Nd-Fe-B	-
Conductivity of magnet	625,000	S/m

III. PM Eddy Current Analysis

In magnetic field analysis, the fundamental equations [8] are given by

$$\nabla \times (v\nabla \times A) = J_0 - \sigma\left(\frac{\partial A}{\partial t} + \nabla\phi\right) \quad (1)$$

$$\nabla \cdot \left[-\partial\left(\frac{\partial A}{\partial t} + \nabla\phi\right)\right] = 0 \quad (2)$$

Where $\boldsymbol{A}$ is magnetic vector potential, ϕ is electric scalar potential, $\boldsymbol{J_0}$ is the magnetizing current density, and v and σ are the magnetic and electric conductivity, respectively.

Fig. 2 presents the magnetic field, eddy current and loss distributions analysis results for each model with armature current 10A at 0 deg current phase angle. The eddy current and loss increase near air-gap due to harmonics of air-gap flux density. Fig. 3 shows the eddy current loss for single PM. The

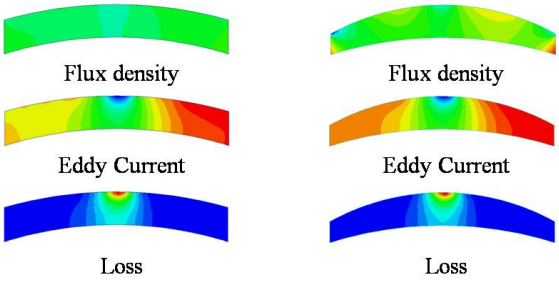

(a) (b)

Fig. 2. Magnetic field and eddy current loss in PM for each model. (a) Model1, (b) Model2

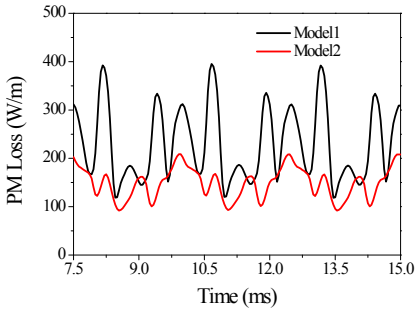

Fig. 3. Eddy current loss for single PM.

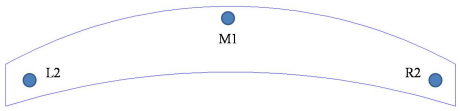

Fig. 4. Definitions of 3-points for field calculation of PM.

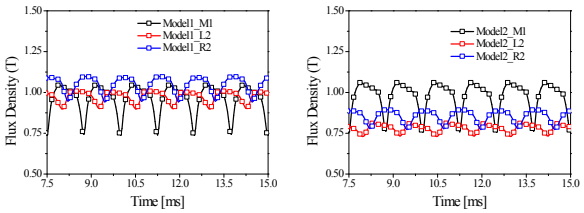

Fig. 5. Flux density curve of each position of PM.

eddy current loss of Model1 is higher than that of Model2 due to harmonics and magnet area.

Fig. 4 presents the three positions in PM to calculate the magnetic field and eddy current. Point M1 is the center point of magnet near air-gap. This is narrowest air-gap length position. Points L2 and R2 are left and right side respectively which are partly enlarged air-gap region. Point L2 is demagnetized region by armature reaction field whereas point R2 is magnetized region. As in Fig. 5, flux density of R2 is higher than that of L2 due to armature reaction effect. Magnetic flux density varies with respect to rotation, so the eddy current induced. Magnetic flux density of point L2 and R2 of Model2 is relatively low due to partly enlarged air-gap, so the eddy current loss can be reduced as in Fig. 3. Fig. 6 and Fig. 7 show the PM eddy current and eddy current loss curve respectively. The eddy current loss at point M1 is highest due to directly affected air-gap flux density harmonics.

Fig. 8 shows the prototype and back EMF measuring result. The detail validation will be displayed in extended paper.

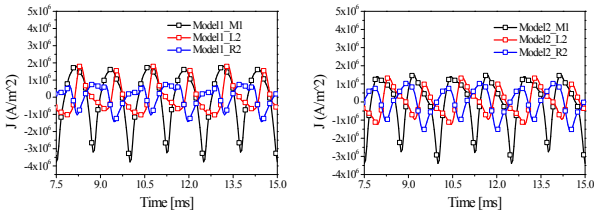

Fig. 6. Eddy current curve of each position of PM.

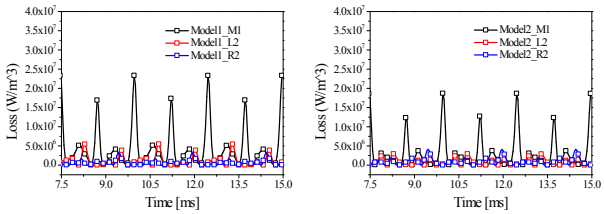

Fig. 7. Loss curve of each position of PM.

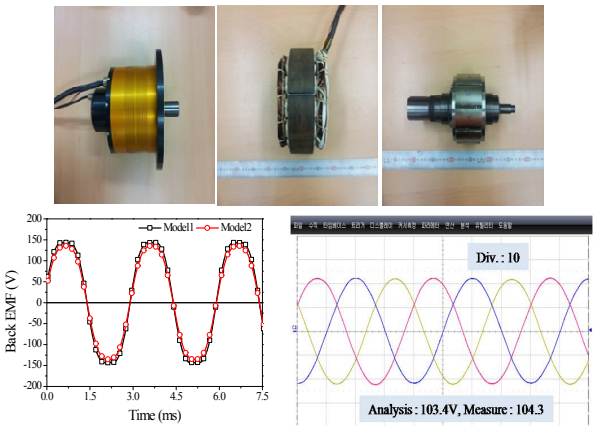

Fig. 8. Prototype of Model2 and back EMF comparison.

REFERENCES

[1] S. -K. Lee, G. -H. Kang, and J. Hur, "Finite element computation of magnetic vibration sources in 100kW two fractional-slot interior permanent magnet machines for ship", *IEEE Trans. Magn.*, vol. 48, no. 2, pp867-870, 2012.

[2] Z. Q. Zhu, D. Ishak, D. Howe, and J, Chen, "Unbalanced magnetic forces in permanent-magnet brushless machines with diametrically asymmetric phase windings", *IEEE Trans. Ind. Appl.*, vol. 43, no. 6, pp1544-1553, 2007.

[3] K. Yamazaki, and Y. Fukushima, "Effect of eddy-current loss reduction by magnet segmentation in synchronous motors with concentrated winding", *IEEE Trans. Ind. Appl.*, vol. 47, no. 2, pp779-788, 2011.

[4] K. Yamazaki, M, Shina, Y, Kanou, M, Miwa, and J, Hagiwara, "Effect of eddy current loss reduction by segmentation of magnets in synchronous motors : difference between interior and surface types", *IEEE Trans. Magn.*, vol. 45, no. 10, pp4756-4759, 2009.

[5] J. Wang, K. Atallah, R. Chin, W. M. Arshad, and H. Lendenmann, "Rotor eddy-current loss in permanent-magnet brushless AC machines", *IEEE Trans. Magn.*, vol. 46, no. 7, pp2701-2707, 2010.

[6] J. H. Seo, D. K. Woo, T. K. Chung, and H. K. Jung, "A study on loss characteristics of IPMSM for FCEV considering the rotating field", *IEEE Trans. Magn.*, vol. 46, no. 8, pp3213-3216, 2010.

[7] K. Yamazaki, and Y. Fukushima, and M. Sato, "Loss analysis of permanent-magnet motors with concentrated windings-variation of magnet eddy-current loss due to stator and rotor shapes", *IEEE Trans. Ind. Appl.*, vol. 45, no. 4, pp1334-1342, 2009.

[8] L. Ye, D. Li, Y, Ma, and B. Jiao, "Design and performance of a water-cooled permanent magnet retarder for heavy vehicles", *IEEE Trans. Eng. Convs.*, vol. 26, no. 3, pp953-958, 2011.